Proceedings of 19th ASM Heat Treating Society Conference, 1-4 November 1999, Cincinnati, Ohio

Experimental Study of Intensive Quenching of Punches

Michael A. Aronov, Nikolai I. Kobasko and Joseph A. Powell
IQ Technologies Inc, Akron, Ohio
David Schwam and John F. Wallace
Case Western Reserve University, Cleveland, Ohio
John H. Vanas
Euclid Heat Treating Co., Euclid, Ohio
William R. Olson
American Punch Co., Cleveland, Ohio

Introduction

The main material properties that determine the performance of the punch are toughness, strength and wear resistance. The strength and toughness are critical in preventing cracking and chipping of the punch under the severe impact of this fabrication process. The wear resistance is required to preserve the cutting edges of the punch, thereby maintaining constant processing parameters and ensuring the dimensional accuracy of the holes. All of these critical properties are affected by the cooling rate during quenching. A faster cooling rate should permit higher hardness levels without compromising the toughness of the punch.

Presently, tool steel punches are oil quenched and tempered. While the performance of the punches is satisfactory, the manufacturer is interested in further improving the useful life of the punches by utilizing a faster cooling rate during the quenching process. The objective of this study was to demonstrate the superior performance of punches quenched by the IntensiQuench^{SM} process. In this process the parts are submersed in a fast flowing jet of quenchant, yielding very fast cooling rates. In addition to the microstructural benefits of the fast cooling rate, the IntensiQuench^{SM} process also generates high compressive stresses at the surface that minimize the risk of quench cracking and extend the useful life of the punches.

Experimental Study

A joint experimental program was initiated to evaluate the effect of IntensiQuench^{SM} process on the properties and performance of S5 steel for punches. The Edison Material Technology Center of Kettering, Ohio funded this program. The participants of the program are IQ Technologies Inc of Akron, Ohio, Euclid Heat Treating Co. of Euclid, Ohio, American Punch Co. and Case Western Reserve University both of Cleveland, Ohio.

Cylinders of 1.5 inches diameter and 2.2 inches long and punches machined from the same steel batch were quenched in oil and by the IntensiQuench^{SM} process. The oil quenching was conducted on batches of punches in a vacuum furnace with a rapid transfer mechanism to an oil quench tank. The IntensiQuench^{SM} process was performed in water on individual cylinders and punches in the IQ Technologies' experimental quenching system described in **References 1** and **2**. In this process, the part is submersed in a flow of water, yielding very fast cooling rates of about 160^{o}F/sec at the surface of the cylinder, as demonstrated by the cooling curves in **Figure 1**. Charpy V-notch samples were cut from the as-quenched and tempered cylinders and evaluated. Hardness measurements were taken from Charpy V-notch samples cut from the cylinders. The distortion of the cylinders was mapped with a Coordinate Measuring Machine.

The depth profile of the residual stresses in the surface region of the cylinders was measured by X-Ray diffraction methods at Lambda Research, Inc. of Cincinnati, Ohio. The X-ray diffraction residual stress measurements were made from the surface to a nominal depth of 0.5mm in approximate increments of 50 x 10^{-3} mm. Measurements were made in the axial and circumferential directions at mid-length of the sample. X-ray diffraction residual stress measurements were performed using a two-angle sine-squared-psi technique, in accordance with SAE J784a, employing the diffraction of chromium K-alpha radiation from the (211) planes of the BCC structure of the S5 steel. The diffraction peak angular positions at each of the psi tilts employed for measurement were determined from the position of the K-alpha 1 diffraction peak separated from the superimposed

K-alpha doublet assuming a Pearson VII function diffraction peak profile in the high back-reflection region. The diffracted intensity, peak breadth, and position of the K-alpha 1 diffraction peak were determined by fitting the Pearson VII function peak profile by least squares regression after correction for the Lorentz polarization and absorption effects and for a linearly sloping background intensity.

Details of the diffractometer fixturing are outlined below:

- Incident beam divergence: 2 deg.
- Detector: scintillation set for 90% acceptance of the Chromium K-alpha energy
- Psi rotation: 10 to 50 deg.
- Irradiated area: 0.1 x 0.3 in. (short axis in the circumferential direction of measurement)

The value of the x-ray elastic constant, $E/(1+\nu)$, required to calculate the macroscopic residual stress from the strain measured normal to the (211) planes of D6AC steel was previously determined empirically. A simple rectangular beam manufactured from D6AC steel loaded in four-point bending on the diffractometer to known stress levels and the resulting change in the spacing of the (211) planes was measured in accordance with ASTM E1426-91. No attempt was made to determine the x-ray elastic constant of the S5 steel employed in the manufacture of the samples.

Material was removed electrolytically for subsurface measurement to minimize possible alteration of the subsurface residual stress distribution as a result of material removal. All data obtained as a function of depth were corrected for the effects of the penetration of the radiation employed for residual stress measurement into the subsurface stress gradient. The stress gradient correction applied to the last depth measured is based upon an extrapolation to greater depths and may result in over correction at the last depth if the stress profile has been terminated in the presence of a steep gradient. Corrections for sectioning stress relaxation and for stress relaxation caused by layer removal are applied as appropriate. The results of this evaluation are discussed in the following section.

Results and Discussion

The hardness of cylinders quenched in oil from 1650°F was 62-63 HRC while the hardness of intensively quenched cylinders from the same temperature was 63-64 HRC. After three hours tempering at 300°F the hardness of all the cylinders was 60-61 HRC as shown in **Table 1.** Hardness measurements were also taken from fourteen Charpy-V-notch samples cut longitudinally from the cylinders.

Table 1 Hardness of Cylinders

Cylinder #	V-notch Sample #	Hardness, HRC
Oil Quenching		
1	1	60.5; 60.1; 60.1
	2	60.1; 60.2; 60.2
	3	60.0; 60.4; 60.5
	4	60.2; 60.8; 60.7
2	1	60.8; 60.6; 60.8
	2	60.8; 60.7; 60.4
	3	60.8; 60.9; 60.9
Average Hardness		60.5
Standard Deviation		0.31
Intensive Quenching		
3	1	60.6; 61.0; 60.5
	2	61.0; 61.0; 61.2
	3	61.1; 61.4; 61.2
4	1	61.1; 61.3; 61.3
	2	60.4; 60.8; 60.7
	3	60.0; 59.6; 59.9
	4	59.4; 59.5; 59.9
Average Hardness		60.6
Standard Deviation		0.65

While the as-tempered average hardness of all the cylinders was practically identical, the oil-quenched specimens were more uniform in hardness with a standard deviation of 0.3 HRC versus a standard deviation of 0.6 in the hardness of the intensively quenched samples. This difference is attributed to the faster heat removal in IntensiQuench[SM] process, which generates a faster cooling rate at the surface relative to the center of the cylinders. The hardness at the surface therefore tends to be slightly higher than in the center.

The toughness levels measured up to 212°F for the cylinders quenched by the IntensiQuench[SM] process were higher than the toughness of the oil quenched cylinders for similar hardness values although both were relatively low because of the high carbon and hardness values of each. The average energy absorbed by the oil quenched Charpy V-notch samples at room temperature was 1 ft·lbf versus 3 ft·lbf for the intensively quenched sample. At 212°F the average energy absorbed by the oil quenched Charpy V-notch was 2.5 ft·lbf versus 4.5 ft·lbf for the intensively quenched sample. The higher toughness at similar hardness levels is an indication of superior performance. It

means the punch should have more resistance to chipping when intensively quenched. Alternatively, intensively quenched punches could be tempered to higher hardness, while still maintaining acceptable toughness levels. This in turn could improve the wear resistance of the punch relative to an oil-quenched punch.

The difference in quenching rates between the oil and the IntensiQuench[SM] process also affects the distortion patterns of the cylinders. The distortion map of an oil-quenched cylinder is shown in **Figure 2**. The arrows indicate the direction and magnitude of the move. The cylinder is bulged around the center perimeter, with the center diameter about 0.0032" *larger* than the top and bottom diameters. The distortion map of an intensively quenched cylinder is shown in **Figure 3**. The cylinder has an "hourglass" shape, with the center diameter being about 0.0032" *smaller* than the sides. These differences can be explained by considering the dimensional changes during the phase transformation. The rapid cooling rate during IntensiQuench[SM] process quickly forms a hard and stiff layer of martensite over the entire surface of the cylinder. The expansion associated with the martensitic transformation causes high compressive stresses at the surface, which are partially accommodated by this change in shape. The top and bottom of the cylinder expand pushing the adjacent envelope outward. At the same time, the longitudinal expansion at the surface is pushing the top and bottom perimeters outward. In the oil-quenched cylinder, the strong martensitic layer does not form so quickly. When the core transforms and expands, it can still push the envelope of the cylinder out, causing it to bulge. These differences are significant in two aspects. The first aspect concerns the dimensional control of the punches, which has to be kept within tolerance. The second aspect relates to the residual stresses. It was anticipated that the IntensiQuench[SM] process would generate higher compressive stresses in the surface thus minimizing the risk of cracking during the quench and the use of the punch. The distortion pattern indicates this is indeed the case.

The axial and circumferential residual stress distributions measured as functions of depth are shown graphically in **Figures 4** and **5**. Compressive stresses are shown as negative values, tensile as positive, in units of MPa. The X-Ray residual stress measurements detected axial and circumferential compressive stresses of 900 MPa at the surface of the intensively quenched cylinders. In the oil quenched cylinders tensile residual stresses of about 200 MPa were measured. For cylindrical samples from which complete shells were removed by electropolishing for subsurface measurement, the radial stress is calculated assuming a rotationally symmetrical residual stress distribution. The error shown for each residual stress measurement is one standard deviation resulting from random error in the determination of the diffraction peak angular positions and in the empirically determined value of $E/(1 + \nu)$ in the <211 > direction. An additional semi-systematic error on the order of $\underline{+2}$ ksi (±14 MPa) may result from sample positioning and instrument alignment errors. The magnitude of this systematic error was monitored using a powdered metal zero-stress standard in accordance with ASTM specification E915, and found to be +10 MPa during the course of this investigation.

Conclusions

IntensiQuench[SM] process of S5 steel cylinders followed by tempering to 60-61 HRC resulted in higher Charpy V-notch toughness at room temperature and 212°F temperature over identical oil quenched cylinders. The main material properties that determine the performance of the punch are toughness, strength and wear resistance. The strength and toughness are critical in preventing cracking and chipping of the punch under the severe impact of this fabrication process. The wear resistance is required to preserve the cutting edges of the punch, thereby maintaining constant processing parameters and ensuring the dimensional accuracy of the holes. All of these critical properties are affected by the cooling rate during quenching. A faster cooling rate feasible with IntensiQuench[SM] process should permit higher hardness levels without compromising the toughness of the punch.

Distortion patterns indicative of higher compressive stresses were measured on the intensively quenched cylinders. The presence of high compressive stresses at the surface of the intensively quenched cylinders was confirmed by detailed X-Ray residual stress depth profiles.

These measurements detected axial and circumferential compressive stresses of 900 MPa at the surface of the intensively quenched cylinders. In the oil quenched cylinders tensile residual stresses of about 200 MPa were measured. The compressive stresses present in the intensively quenched cylinders and punches minimize the risk of cracking during the quench and the use of the punch.

Ultimately, any gain to be made by utilizing the IntensiQuench[SM] process has to be demonstrated at the customer site. With this in mind, batches of identical punches were processes by the two methods and provided to select users. The performance of these punches is currently being monitored and recorded. The integration of the laboratory testing and the field evaluation will

provide a documented justification of the benefits of the IntensiQuench[SM] process.

References

1. Aronov, M. A., Kobasko, N. I., Wallace, and J. F., Schwam, D., "Intensive Quenching Technology for Steel Parts," Proceeding of The 1998 Heat Treating Conference, Chicago, 1998.

2. Aronov, M. A., Kobasko, N. I., Powell, J.A., Wallace, and J. F., Schwam, D., "Practical Application of the Intensive Quenching Technology for Steel Parts," Industrial Heating Magazine, April 1999, pp. 59-63.

Figure 1: Cooling Curves During Intensive Quenching of Cylinder

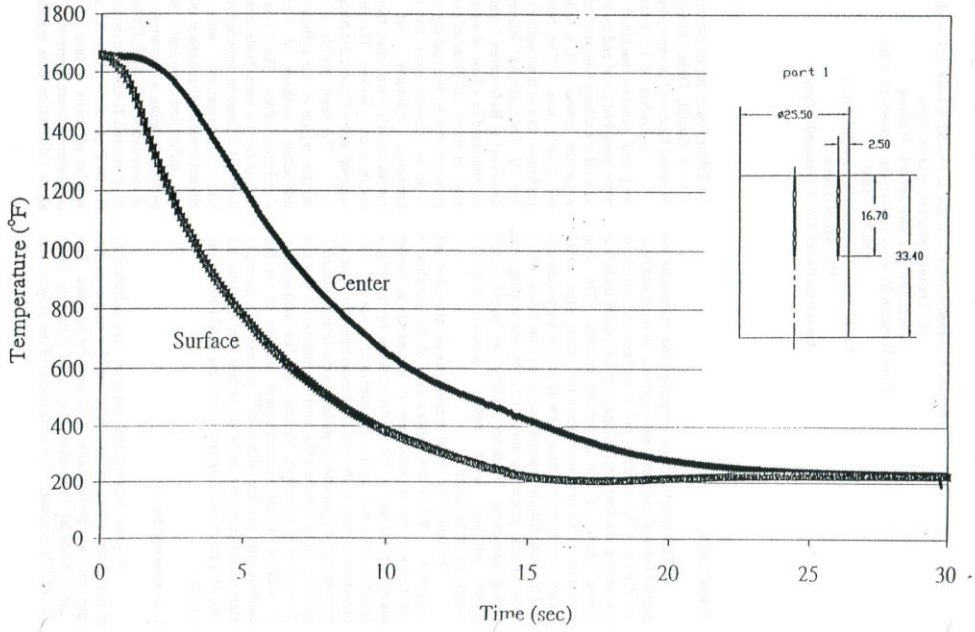

Figure 2: Distortion Map of Oil Quenched Cylinder

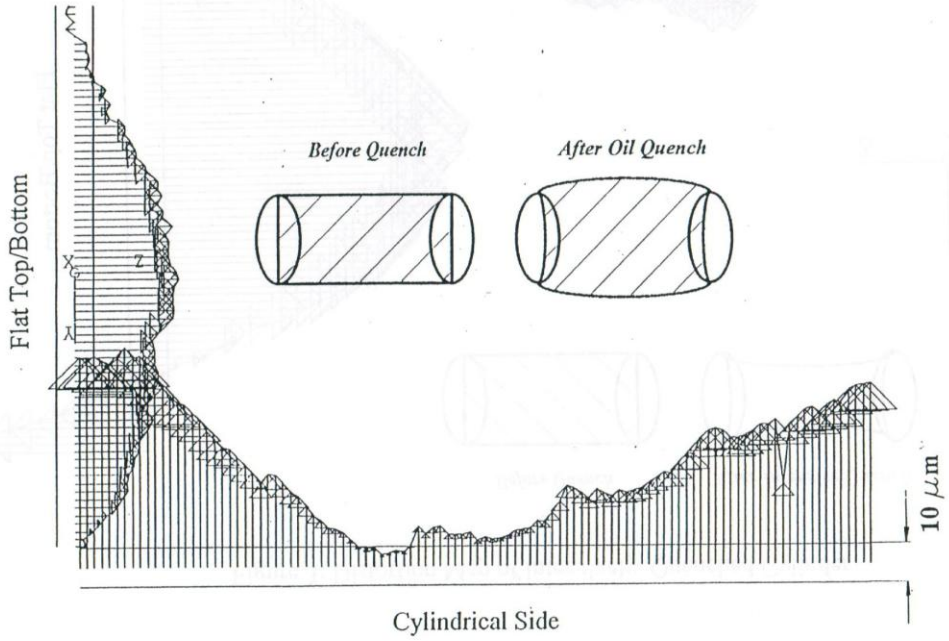

Figure 3: Distortion Map of Intensively Quenched Cylinder

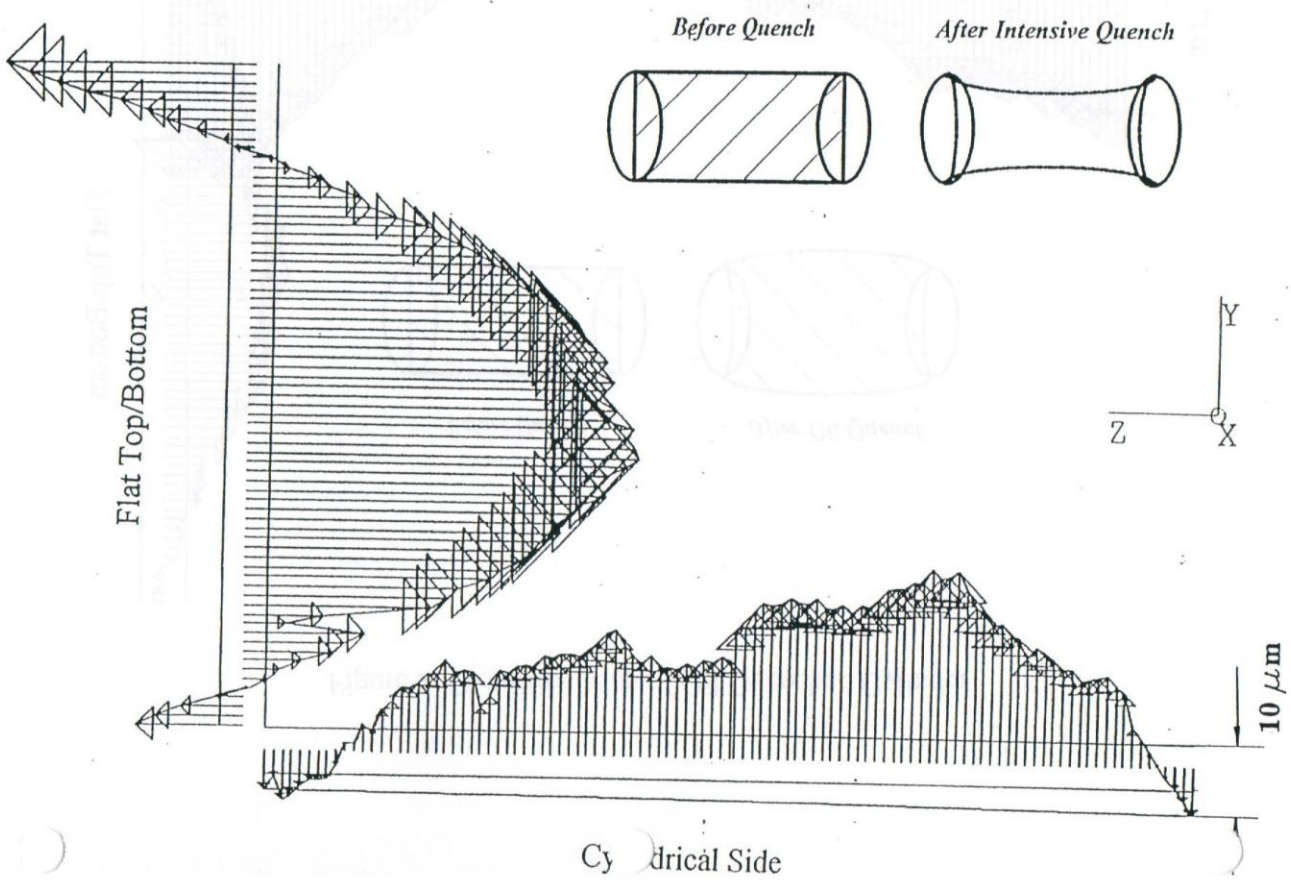

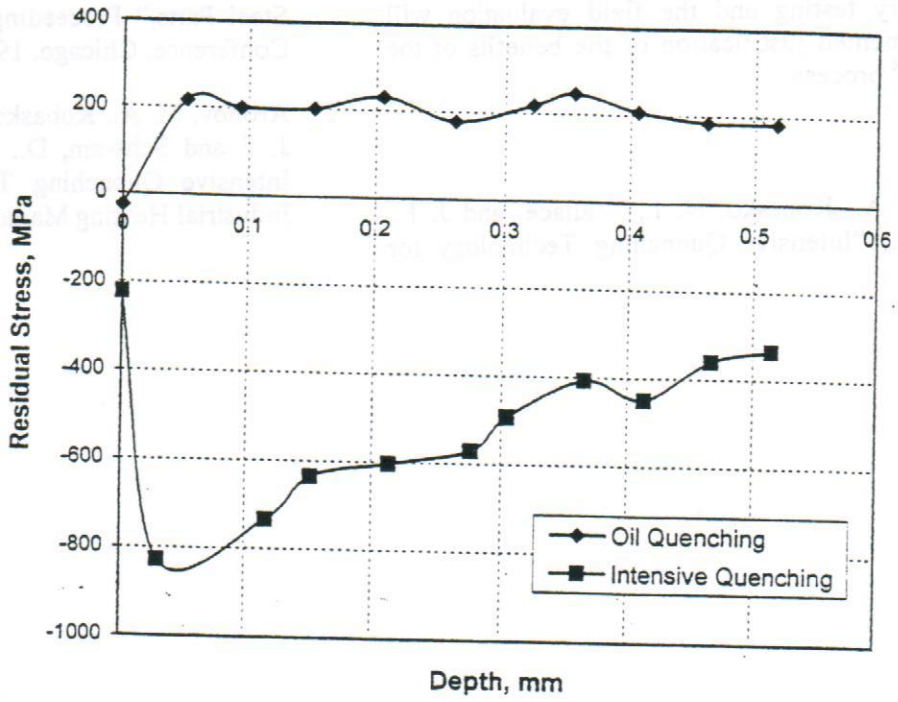

Figure 4 Punch Axial Residual Stresses

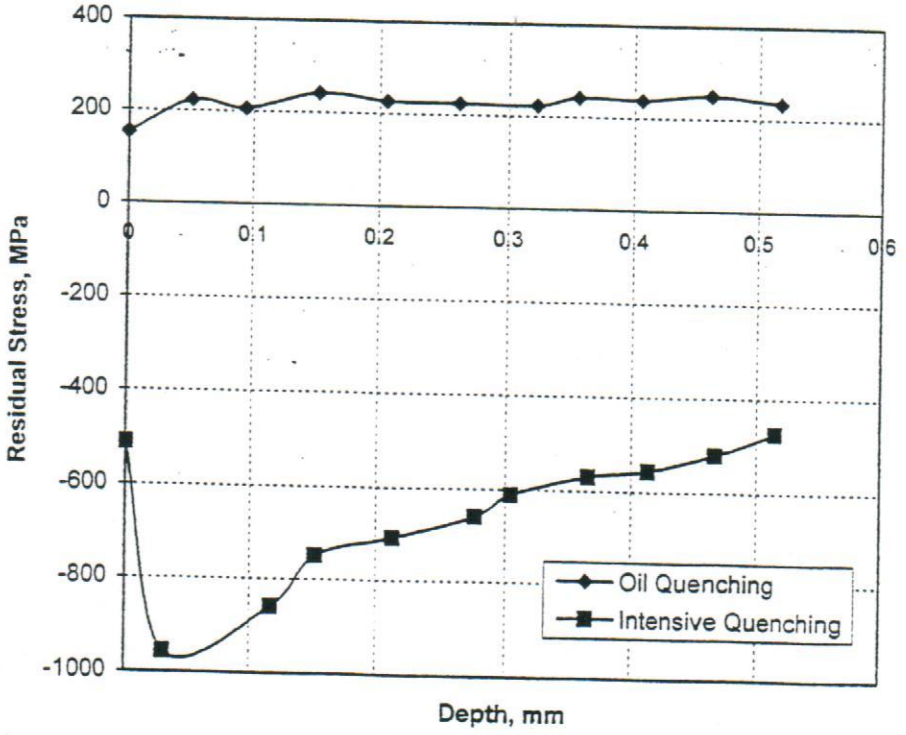

Figure 5 Punch Circumferential Residual Stresses